

Structure and electrochemical properties of nickel hydroxide electrodes with cobalt additives

Xiaofeng Li · Shumian Li · Jiayong Li ·
Huichao Dong

Received: 10 May 2008 / Accepted: 2 October 2008 / Published online: 12 October 2008
© Springer Science+Business Media B.V. 2008

Abstract In this article, cobalt additives are introduced into nickel hydroxide electrodes by two incorporation methods—co-precipitated cobalt hydroxide during the nickel hydroxide synthesis or post-added CoO with nickel hydroxide. The results of X-ray diffraction, cyclic voltammetry, electrochemical impedance spectroscopy, and charge–discharge tests indicate that (i) the diffraction peaks show a decrease in intensity and increase in the half peak breadths for Ni(OH)₂ with co-precipitated cobalt hydroxide; (ii) the electrochemical activity of nickel hydroxide can be improved by both incorporated cobalt and the effects of post-added CoO are more notable; (iii) CoOOH derived from post-added CoO is not stable in the KOH electrolyte when the potential of the Ni(OH)₂ electrode is lowered and its reduction product may be inactive, thus results in an irreversible capacity loss of nickel-metal-hydride battery after over-discharge-state storage.

Keywords Nickel hydroxide electrode · Cobalt additive · Incorporation way · Structure · Electrochemical property

1 Introduction

Pasted nickel hydroxide electrodes with nickel foams as the substrates are widely used in secondary nickel-based alkaline batteries such as nickel–cadmium (Ni–Cd) batteries, nickel-metal-hydride (Ni–MH) batteries and nickel–

zinc (Ni–Zn) batteries. In these Ni(OH)₂ electrodes, cobalt hydroxide is currently used as an additive because of its beneficial effects on electrode performance, for example, enhancement of electrode conductivity [1–3] and a better chargeability [4–6]. Cobalt incorporation to the Ni(OH)₂ electrode is usually realized either by chemical substitution for nickel in the crystal lattice during the Ni(OH)₂ synthesis (e.g., co-precipitation), or by addition of a cobalt-based compound to nickel hydroxide when preparing the admixture to be pasted into a nickel foam (post-addition).

Usually both post-added cobalt and co-precipitated cobalt are used in the pasted Ni(OH)₂ electrodes. V. Pralong et al. [7] reported different oxidation behaviors on them: for post-added cobalt, oxidation of Co (II) occurs at 0.9 V vs. Cd/Cd(OH)₂; but for co-precipitated one, no specific oxidation signature is observed. In this article, post-added CoO and co-precipitated cobalt hydroxide are incorporated to the pasted Ni(OH)₂ electrodes, respectively. Their contribution to the structure and electrochemical performance of nickel hydroxide is studied through X-ray diffraction (XRD), cyclic voltammetry (CV), electrochemical impedance spectroscopy (EIS), and charge–discharge measurements.

2 Experimental

1 mol L⁻¹ mixed solutions of nickel sulfate with 0 wt.% (A), 3 wt.% (B), or 6 wt.% (C) cobalt sulfate were separately dropped into a 2 mol L⁻¹ sodium hydroxide solution under magnetic stirring at 50 °C. The green precipitates were aged at 20 °C for 24 h, then filtered, washed with distilled water, dried at 120 °C and grinded to obtain three kinds of nickel hydroxide. The contents of cobalt hydroxide in nickel hydroxide were tested using an IRIS advantage inductively coupled plasma (ICP) spectroscopy.

X. Li (✉) · S. Li · J. Li · H. Dong
Henan Provincial Key Laboratory of Surface and Interface,
Zhengzhou University of Light Industry, Zhengzhou 450002,
China
e-mail: lixiaofeng@zzuli.edu.cn

A commercial $\text{MmNi}_{3.55}\text{Co}_{0.75}\text{Al}_{0.2}\text{Mn}_{0.5}$ (AB_5) alloy and $\text{Ni}(\text{OH})_2$ obtained above were used in this article. A slurry containing 98 wt.% AB_5 alloy powder and 2 wt.% polyvinyl alcohol (PVA) binder was pasted into a nickel foam, dried, and compressed to obtain negative MH electrodes. Four kinds of positive $\text{Ni}(\text{OH})_2$ electrodes were prepared by filling a nickel foam with a mixture of 2 wt.% polytetrafluoroethylene (PTFE) binder, 10 wt.% metal nickel powder and 88 wt.% $\text{Ni}(\text{OH})_2$ (A, B, or C), respectively, or a mixture of 2 wt.% PTFE binder, 6 wt.% CoO , and 93 wt.% $\text{Ni}(\text{OH})_2$ (A), also dried and compressed.

CV and EIS tests of these $\text{Ni}(\text{OH})_2$ electrodes were performed using a Solartron Electrochemical Interface model SI1287. A three-compartment electrolysis cell was used for the measurements. Two MH counter electrodes were placed on both sides and the working electrode was positioned at the center. A $\text{Hg}/\text{HgO}/\text{OH}^-$ (7 mol L^{-1} KOH) reference electrode was used with a luggin capillary in the region of the working electrode.

The negative electrodes and positive electrodes were assembled with the polypropylene separators to form AA type batteries. A 7 mol L^{-1} KOH electrolyte was poured therein. The batteries were then sealed and placed in a thermoregulated room at 20°C , charged initially at a 0.1 C rate for 15 h and discharged at a 0.2 C rate to a cut-off voltage 1.0 V. Here C corresponds to the current needed to discharge the total capacity of the batteries in 1 h. Afterward, a cycling test was performed on the batteries by charging at a 0.2 C rate for 7 h and discharging at the same rate to a cut-off voltage 1.0 V for stabilizing their capacity.

Afterwards the batteries were discharged at a 0.1 C rate to a cut-off voltage 1.0 V, and then were electrically loaded with an external 2Ω resistor and stored at 60°C for 7 days as imposing over-discharge on the batteries [8]. After storage, a cycling test was performed again on the batteries as the way prescribed above.

The sealed batteries before and after storage were destroyed and the active materials of the positive electrodes were dissociated from the nickel foam substrates by using an ultrasonic oscillator, then filtered, washed with distilled water and dried for XRD analyses using a D/max 2,550 V diffractometer equipped with a graphite monochromator and Cu K_α radiation.

3 Results and discussion

The results of the ICP spectroscopy tests show that the contents of cobalt hydroxide in three kinds of nickel hydroxide are 0, 2.99, and 5.98 wt.% respectively, which means a complete co-precipitation of cobalt with nickel during the preparation of nickel hydroxide. Figure 1 shows XRD patterns of the active materials of the $\text{Ni}(\text{OH})_2$

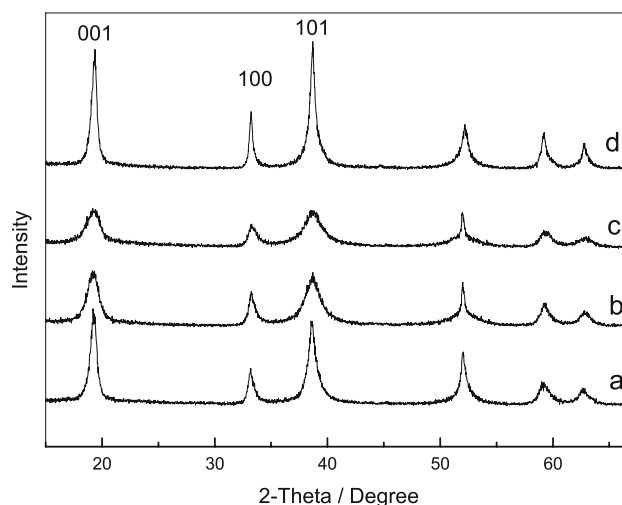


Fig. 1 XRD patterns of active materials of $\text{Ni}(\text{OH})_2$ electrodes before storage: **a** without cobalt additive, **b** with 3 wt.% co-precipitated cobalt hydroxide, **c** with 6 wt.% co-precipitated cobalt hydroxide, and **d** with 6 wt.% post-added CoO

electrodes before storage. Compared to the active material without any cobalt additive (Fig. 1a), a structure of $\beta\text{-Ni}(\text{OH})_2$ is maintained for both the active materials with co-precipitated cobalt hydroxide (Fig. 1b and c) and post-added CoO (Fig. 1d). But intensity of the diffraction peaks decreases markedly and the half peak breadth of {101} crystal plane increases from 0.827° (Fig. 1a) to 1.608° (Fig. 1b) and 1.735° (Fig. 1c), which indicates a crystallinity reduction of nickel hydroxide since the crystal defects increase with the substitution of cobalt for nickel in the crystal lattice. On the other hand, as post-added CoO dissolves in the electrolyte, forming a deep blue complex, and then upon the first oxidation $\beta\text{-CoOOH}$ precipitates on the surface of nickel hydroxide particles [1], its structure may be similar to the latter thus the diffraction peaks of the active material (Fig. 1d) shows little change.

CV tests of the $\text{Ni}(\text{OH})_2$ electrodes were performed with a scanning range between -0.90 and 0.65 V. As shown in Fig. 2a, for the $\text{Ni}(\text{OH})_2$ electrode without any cobalt additive, two peaks (P_1 and P_2) corresponding to the oxidation/reduction between $\text{Ni}(\text{OH})_2$ and NiOOH emerge at about 540 and 280 mV, respectively, and no reaction is found between 0 and -0.90 V. Similar cyclic voltammograms are observed for the $\text{Ni}(\text{OH})_2$ electrodes with co-precipitated cobalt hydroxide as reported in Fig. 2b and c. But for the $\text{Ni}(\text{OH})_2$ electrode with post-added CoO (Fig. 2d), during the first cycle, CoO is oxidized to CoOOH with an oxidation peak (P_3) at about 189 mV, followed with the oxidation/reduction between $\text{Ni}(\text{OH})_2$ and NiOOH , then CoOOH is reduced to Co(II) with a reduction peak (P_4) at about 87 mV. The reduction of CoOOH seems to be irreversible since the reduction peak current is only 56% of the oxidation one in the 1st cycle and both the

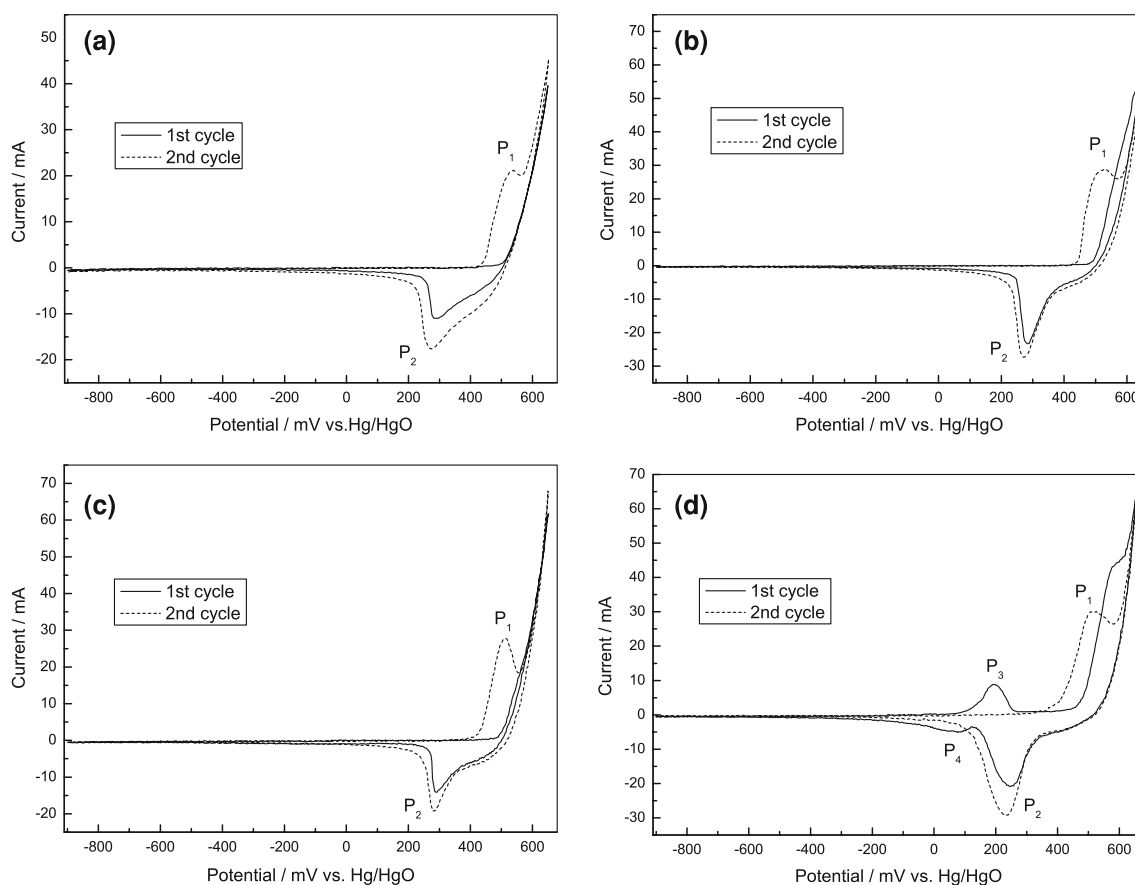


Fig. 2 Cyclic voltammograms for pasted $\text{Ni}(\text{OH})_2$ electrodes (area = 1 cm^2 , loading = 150 mg cm^{-2}) in 7 mol L^{-1} KOH electrolyte between -0.90 and 0.65 V at a scanning rate of 0.25 mV s^{-1} : **a** without any cobalt additive, **b** with $3 \text{ wt.}\%$ co-precipitated cobalt hydroxide, **c** with $6 \text{ wt.}\%$ co-precipitated cobalt hydroxide, and

d with $6 \text{ wt.}\%$ post-added CoO. P_1 is current peak for oxidation of $\text{Ni}(\text{OH})_2$ to NiOOH , P_2 is current peak for reduction of NiOOH to $\text{Ni}(\text{OH})_2$, P_3 is current peak for formation of CoOOH , and P_4 is current peak for reduction of CoOOH

redox peaks disappear in the 2nd cycle. Based on these results, it can be concluded that CoOOH derived from post-added CoO is not stable at lower potential in the KOH electrolyte [8] and its reduction product may be inactive.

Figure 3 shows impedance plots of the pasted $\text{Ni}(\text{OH})_2$ electrodes discharged to 100% depth of discharge. Clearly, the plots exhibit two arcs in the whole frequency range. It is known that the semicircle at high frequency regions corresponds to the charge transfer resistance (R_{ct}) in parallel connection with the double layer capacitance (C_{dl}) and the line at low frequency regions corresponds to the Warburg impedance (Z_w) of proton diffusion [9]. A proposed equivalent circuit for the frequency response of the $\text{Ni}(\text{OH})_2$ electrode is given in Fig. 4, where R_s corresponds to the solution resistance. Table 1 lists the parameters (R_{ct} and C_{dl}) related to the surface properties of the active materials obtained by fitting experimental data according to the equivalent circuit. Decrease in R_{ct} and increase in C_{dl} indicate that the surface electrochemical activity of nickel

hydroxide can be improved by both incorporated cobalt additives. The effects of post-added CoO are particularly notable since $\beta\text{-CoOOH}$ coated on the surface of nickel hydroxide particles has higher electrical conductivity than NiOOH [1].

Figure 5 shows typical charge–discharge curves of the sealed Ni–MH batteries with different $\text{Ni}(\text{OH})_2$ electrodes. For the batteries with co-precipitated cobalt hydroxide, both the charge and discharge voltage decrease and the capacity increases because of a better redox reversibility between $\text{Ni}(\text{OH})_2$ and NiOOH by the substitution of cobalt for nickel [10]. But as cobalt hydroxide is not involved in the normal charge–discharge reactions of the $\text{Ni}(\text{OH})_2$ electrodes, excessive co-precipitation (e.g., $6 \text{ wt.}\%$) results in a lower capacity (Fig. 5c). For the battery with post-added CoO, its capacity markedly increases and the charge voltage decreases since $\beta\text{-CoOOH}$ with higher electrical conductivity is coated on the surface of nickel hydroxide. These results indicate that differently incorporated cobalt

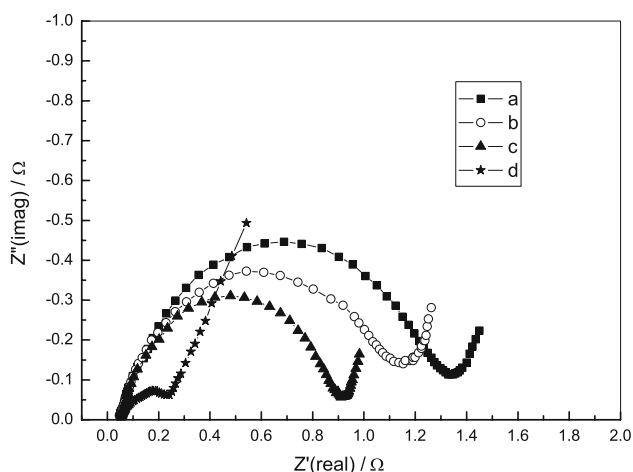


Fig. 3 Impedance plots of pasted Ni(OH)₂ electrodes (area = 1 cm², loading = 150 mg cm⁻²) discharged to 100% depth of discharge in 7 mol L⁻¹ KOH electrolyte at a frequency range from 10⁵ to 10⁻² Hz: **a** without any cobalt additive, **b** with 3 wt.% co-precipitated cobalt hydroxide, **c** with 6 wt.% co-precipitated cobalt hydroxide, and **d** with 6 wt.% post-added CoO

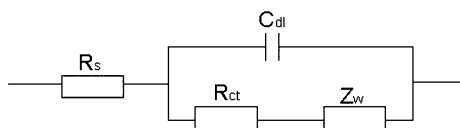


Fig. 4 Proposed equivalent circuit for Ni(OH)₂ electrode

Table 1 Impedance parameters of pasted Ni(OH)₂ electrodes in 7 mol L⁻¹ KOH electrolyte

	R_{ct}/Ω	C_{dl}/F
Electrode without cobalt additive	1.346	0.0946
Electrode with 3 wt.% co-precipitated cobalt hydroxide	1.174	0.109
Electrode with 6 wt.% co-precipitated cobalt hydroxide	0.903	0.141
Electrode with 6 wt.% post-added CoO	0.251	0.508

additives have different beneficial effects on the electrochemical properties of Ni-MH batteries.

An irreversible capacity loss (18.1%) is observed on the battery with post-added CoO after storage as shown in Table 2. On the contrary, no significant capacity loss happens on the batteries with co-precipitated cobalt hydroxide or without any cobalt additive. This is consistent with the results of CV tests mentioned above as CoOOH derived from post-added CoO is not stable at lower potential and its reduction product may be inactive. Figure 6 shows XRD patterns of the active materials of the Ni(OH)₂ electrodes after storage. As compared to Fig. 1d, new diffraction peaks appear at $d = 4.41$ and 1.43 for the

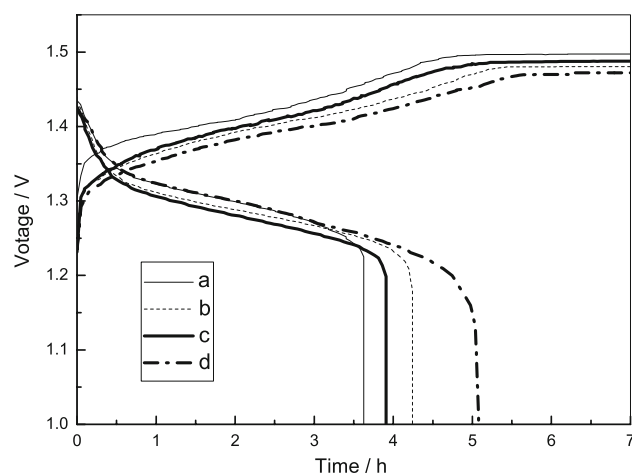


Fig. 5 Typical charge/discharge curves of Ni-MH batteries at a 0.2 C rate before storage: **a** without any cobalt additive, **b** with 3 wt.% co-precipitated cobalt hydroxide, **c** with 6 wt.% co-precipitated cobalt hydroxide, and **d** with 6 wt.% post-added CoO

active material with post-added CoO (being marked with the asterisks in Fig. 6d), which indicates the formation of a new material with different structure to nickel hydroxide. These diffraction peaks are identified to be related to a cobalt compound CoO(OH) by Powder Diffraction File of JCPDS with card number 14-0673. This CoO(OH) is different to β -CoOOH obtained during the first charge of the batteries as it no longer has a structure similar to nickel hydroxide. Its electrochemical activity is poor as shown in Fig. 2d, thus the surface electrochemical activity of Ni(OH)₂ is lowered and leads to the irreversible capacity loss of the batteries.

4 Conclusion

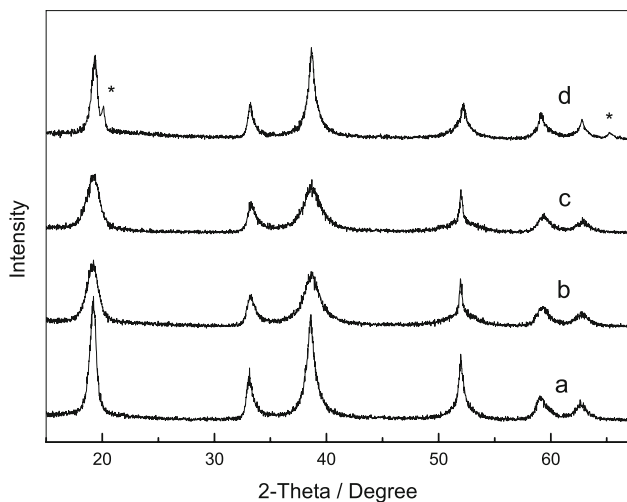
Nickel hydroxide electrodes either with co-precipitated cobalt hydroxide or post-added CoO are prepared in this article and the structure of the active materials is studied by XRD. The diffraction peaks show a decrease in intensity and increase in half peak breadths for Ni(OH)₂ with co-precipitated cobalt hydroxide. On the other hand, CoOOH derived from post-added CoO has little effect on the structure of the active material.

The surface electrochemical activity of nickel hydroxide can be improved by both incorporated cobalt and the effects of post-added CoO are more notable, but CoOOH derived from post-added CoO is not stable at lower potential in the KOH electrolyte and its reduction product may be inactive by using CV and EIS tests.

Differently incorporated cobalt additives have different beneficial effects on the electrochemical properties of the Ni-MH batteries. The capacity of the battery with post-added CoO markedly increases but shows an irreversible

Table 2 Capacity of Ni-MH batteries before and after storage

	Capacity before storage/mAh	Capacity after storage/mAh			
		Cycle 1	Cycle 2	Cycle 3	Cycle 4
Electrode without cobalt additive	1,138	1,092	1,135	1,132	1,130
Electrode with 3 wt.% co-precipitated cobalt hydroxide	1,330	1,281	1,332	1,335	1,336
Electrode with 6 wt.% co-precipitated cobalt hydroxide	1,226	1,177	1,230	1,233	1,238
Electrode with 6 wt.% post-added CoO	1,602	1,211	1,310	1,312	1,312

**Fig. 6** XRD patterns of active materials of Ni(OH)₂ electrodes after storage: **a** without cobalt additive, **b** with 3 wt.% co-precipitated cobalt hydroxide, **c** with 6 wt.% co-precipitated cobalt hydroxide, and **d** with 6 wt.% post-added CoO

loss after over-discharge-state storage. An inactive CoO(OH) is observed and may be responsible for the irreversible capacity loss.

References

- Oshitani M, Yufu H, Takashima K et al (1989) *J Electrochem Soc* 136:1590
- Pralong V, Delahaye-Vidal A, Beaudoin B et al (2000) *J Electrochem Soc* 147:1306
- Butel M, Gautier L, Delmas C (1999) *Solid State Ion* 122:271
- Bronoel G, Reby J (1980) *Electrochim Acta* 25:973
- Ding Y, Yuan J, Chang Z (1997) *J Power Sources* 69:47
- Oshitani M, Sasaki Y, Takashima K (1984) *J Power Sources* 12:219
- Pralong V, Chabre Y, Delahaye-Vidal A et al (2002) *Solid State Ion* 147:73
- Lichtenberg F, Kleinsorgen K (1996) *J Power Sources* 62:207
- Cheng S, Leng W, Zhang J et al (2001) *J Power Sources* 101:248
- Provazi K, Giz MJ, Dall'Antonia LH et al (2001) *J Power Sources* 102:224